

Conduction Electron Resonance and Transport Properties of a Nonaligned Carbon Nanotube Thick Film for Field Emission Display

Yun-Hi Lee,^{a,z} Hoon-Kim,^a Dong-Ho Kim,^b and Byeong-Kwon Ju^a

^a*Korea Institute of Science and Technology, Cheongryang, Seoul, Korea*

^b*Yeungnam University, Kyongsan, Korea*

We present electron spin resonance spectra and the electronic transport characteristics of multiwalled carbon nanotubes (CNTs) which were screen printed in a thick-film form for field emission displays. Electron spin resonance spectra showed a Dysonian line due to conduction electrons, and the reduced temperature dependence of the g -value indicates the metallic properties of CNTs. Zero-field resistivity and magnetoresistance were measured as a function of temperature T in the range 1.7–390 K and magnetic field, respectively. The resistivity of nanotubes for temperatures of 10–390 K indicates that the system is intrinsically metallic and the characteristics are well described by Mott's $T^{-1/4}$ law in temperatures above 10 K. We found that the main contribution to the conductivity comes from carriers that hop directly between localized states via variable range hopping. The temperature dependence above 10 K is in good agreement with that of an individual multiwalled CNT. However, below 10 K, the resistivity is well fit to Efros' $T^{-1/2}$ law, confirming the presence of a coulomb gap for the system. With a decrease of the temperature below 10 K the charge carriers in the system are localized by strong disorder, bringing a nearly insulating state. Using a diode configuration, we measured the field electron emission characteristics and found that the CNT thick film appears to emit electrons with a density of $80 \mu\text{A}/\text{cm}^2$, accompanying highly bright light emission. The emission current-voltage characteristics can be fitted to a straight line in agreement with the Fowler-Nordheim equation, which confirms that the emission current resulted from field emission of the CNT thick film.

© 2000 The Electrochemical Society. S0013-4651(00)01-109-5. All rights reserved.

Manuscript submitted January 26, 2000; revised manuscript received May 18, 2000.

Following their discovery,¹ carbon nanotubes (CNTs) attracted much attention due to their extraordinary properties and possibilities for various applications, *i.e.*, in electronic, medical, or chemical fields. Specific electronic, magnetic, or mechanical properties can be expected for these quasi one-dimensional nanomaterials. Though the potential applications of CNTs in nanotechnology are for the moment speculative, production and purification of CNTs having controlled structural and electrical characteristics will probably be realized in the near future.

Due to high aspect ratio and small tip radii of curvature, CNTs may be suitable for electron field emission under high fields²⁻⁹ and therefore, great attention has been paid to field emission of multiwalled carbon nanotubes (MWNTs) due to their long-term stability and mechanical strength as compared to those of single-wall nanotubes. The MWNT-rich material is deposited on the cathode electrode by the arc-deposition method and a subsequent treatment is required in order to utilize the MWNTs for electron emitter applications. The electronic properties of MWNTs are of great interest, but they also appear to be the most challenging to measure. Very recently, it has become possible to make a four-probe measurement on an individual CNT and to accurately evaluate the electric properties of a single CNT.¹⁰⁻¹⁵ After the first such report, there have been a few studies on the electrical characteristics of the MWNT systems such as individual, thin-film form, and sheet form.¹⁶⁻²⁰ At the same time, much has been learned from other types of measurements. For instance, electron spin resonance (ESR) studies indicate that a fraction of the CNTs are indeed metallic, narrow-band semiconductor, or wide bandgap semiconductor depending on defects in CNTs, which must be annealed away through acid and heat-treatment.

Though several studies were performed to identify specific characteristics of an individual CNT, CNTs as an electron source for field emission display are generally formed as a thin sheet. In this case, CNTs are typically mixed with conductive paste, and until now, only their field-emission properties under high electric field of $\text{V}/\mu\text{m}$ were reported. It is easily expected that the CNTs mixed with conducting paste may induce severe deviation from properties of an individual CNT, resulting in complex behaviors.

This work presents a detailed study of the structural and electrical properties of both purified MWNTs of the main matrix material

and a thick-film form MWNT mixed with conductive paste for field electron emitters. We focus on the comparison of the properties between an individual MWNT reported by others and our thick-film form MWNTs, which are assumed to be promising cathode emitters for large area display. The resulting properties are discussed.

Experimental

The starting raw CNT materials were produced by arc deposition (Iljin Co., Korea). Three batches (2 g) of MWNT raw deposits were first placed on an alumina plate, then heated to 600°C for 30 min under normal atmosphere. After initial firing, the powders were removed from the furnace, then weighed and regrounded in ethanol using ultrasonic cleaner. In order to remove metallic impurities, the MWNT powders were immersed in HNO_3 for 5 min, then rinsed in deionized water, several times. The purified CNT powder was mixed with conductive binder (silver epoxy) with a volume ratio of 1:1 using a stirrer. Then 20 μm thick CNT film was formed by the silk screen method on the bare glass substrate for the four-probe measurements and Cr-coated 2×3 cm glass substrate for field emission study, respectively.

ESR spectra were recorded using a Bruker ESP-300S spectrometer operating at 9.8 GHz equipped with a variable temperature accessory. Electrical resistivity was measured using the conventional four-probe method in the temperature range 1.7–390 K. For electrical contacts, four Al pads were formed by thermal evaporation and then highly conducting graphite adhesive was used for contacting Al and wiring Au. The ohmic contact down to the lowest temperature was confirmed by checking the linear relationship between voltage and current. The resistivity was measured using a Keithley 220 programmable current source and 182 nanovoltmeter. The temperature dependence of resistivity and magnetoresistance (MR) as a function of temperature were measured in fields up to 5.5 T using a He⁴ cryostat equipped with a superconducting magnet (Quantum Design). Based on these analyses, we suggest what is the dominant conduction mechanism in the measured temperature range and discuss the differences of the electrical conduction characteristics between the thick-film MWNTs and an individual MWNT or their sheet form reported previously.

Field electron emission properties under the strong electric field were measured on the thick-film MWNTs on a soda-lime glass sub-

^z E-mail: lyh@kist.re.kr

strate predeposited with Cr electrodes for the cathode. The spacing between greenish-blue light emitting ZnO:Zn phosphor-coated indium-tin oxide (ITO) glass and the MWNT cathode was fixed at 100 μm using glass fiber spacers.

Results and Discussion

ESR results.—The ESR studies of CNT reveal many aspects of the material and also illustrate very well the issue of defects and sample preparation. Zhou *et al.* reported a very weak ESR signal for an unpurified nanotube (NT) with a g -value of 2.000, while Kosaka *et al.*²¹ observed a strong conduction ESR signal for unpurified and purified NT indicating the presence of metallic and/or narrow-band gap semiconducting CNTs. The effect of the annealing can also be seen by comparing the intensity and g -value dependence of conduction ESR peaks for purified and purified annealed NTs, as shown in Fig. 1a and b. At room temperature, ESR spectra for the unpurified sample is clearly composed of two signals, a narrow signal (A) and a broader one (B). There is some uncertainty in the estimation of the linewidth of B, because its intensity is lower than that of the narrow signal. These two signals are characteristic of an inhomogeneous material²² containing broad signal and narrow signal. The B signal vanished continuously when the temperature decreased, then at 125 K, it is very small in ESR spectrum. Here, we tentatively suggest that the A signal is related to the resonance centers in graphite carbon existing in the CNT network.

For the purified CNT, the signal intensity in Fig. 1b decreased one half the value of the unpurified one and also, signal A disappeared and an asymmetric line appeared, showing the trace of signal A. This, called the Dysonian,²⁴ may originate from the motion of paramagnetic centers as well as a motional narrowing effect due to active hopping of the electrons after the purification. In purified

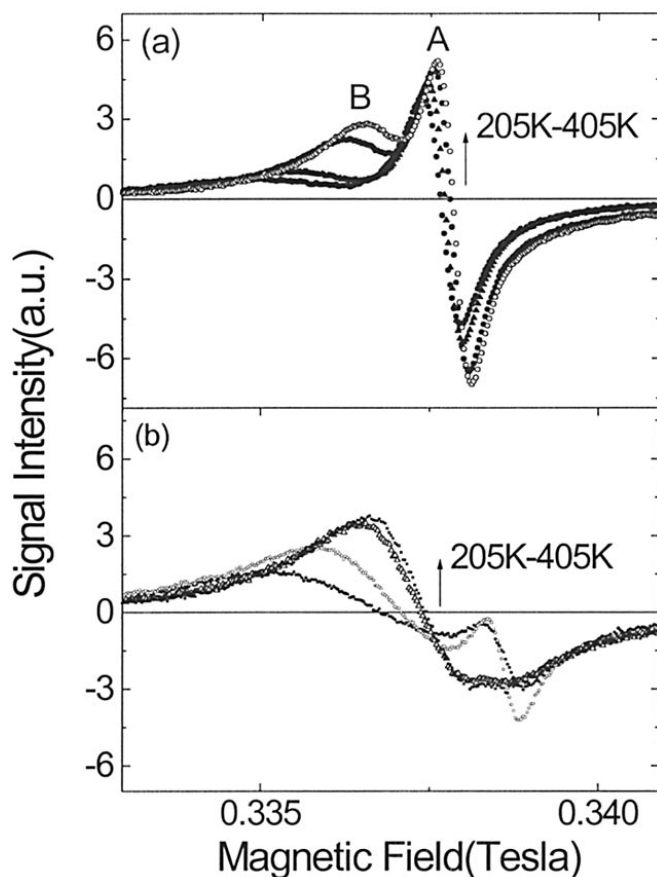


Figure 1. The temperature dependence of EPR spectra for the MWNTs. The resonance signal shows a Dysonian shape and corresponds to the typical signal due to conduction electrons: (a) unpurified CNTs and (b) purified sample, respectively.

CNTs, the collapse of two signals which were observed in unpurified CNTs indicates the fact that more homogenous material resulted from purification.

The measured g -value of the CNTs after purification in Fig. 2 showed a nearly constant value at measuring temperature range of 125-405 K, as compared to that of the unpurified one. The fact that the g -value of the purified CNT sample becomes temperature independent upon purification can be understood if the large portion of our CNTs have closed cylindrical structures, which was confirmed by transmission electron microscopy (TEM) images. If the open tubes are dominant, the interlayer spacing and therefore interlayer interactions are more temperature dependent. Finally, we have to reconsider the dependence of the signal intensity on the relative spin carrier concentration (*i.e.*, intensity) as considering I (signal intensity) $- N$ (spin density) $\times \delta_c$ (skin depth). Considering the fact that the number of spins present in the CNTs is directly related to the area of the absorption signal, the decrease of signal intensity indicates the removal of graphite carbon and other carbonaceous particles, which was one of the resonance centers, after purification. On the other hand, such a purification treatment can also lead to modifications of the spin interactions, which induces a decrease of the frequency of the electron-electron and electron-phonon collisions, and as a result the conductivity relaxation time (or diffusion time τ) increases. Therefore, we expect a decrease of resistivity for the purified CNTs which is confirmed through the measurement of electrical resistivity.

Electronic transport and field electron emission characteristics.

Figure 3a shows the changes in resistance, R , which were measured as a function of temperature over 1.7–390 K range for the thick-film form MWNT samples with an average external diameter of 15–30 nm. It is found that the resistance increases rapidly below 100 K and is nearly constant between 100 and 360 K and also increases with increasing temperature above 360 K. For different thick-film MWNT samples with a different external diameter of 25–60 nm, nearly the same trend was observed as shown in Fig. 3b.

The resistance vs. temperature in the range $1.9 \text{ K} < T < 100 \text{ K}$ was measured more precisely using four Al contacts in the plane of the MWNT sheet mixed with conductive binder. Figure 4a shows the resistance of the MWNT plotted logarithmically against $T^{-1/2}$ and in Fig. 4b, against $T^{-1/4}$ over the higher temperature range. The MWNT obeys an $x = 1/4$ ($x: T^{-x}$) variable range hopping (VRH) law²⁶⁻²⁸ from 10 to 100 K. This is shown in Fig. 2b and clearly, a single line does not fit the data over the entire temperature range of 1.9–100 K. On the other hand, the linear dependence of $\ln [R(T)]$ on $T^{-1/2}$, as shown in Fig. 4a, indicates that Efros and Shklovskii (ES) VRH conduction²⁸ slightly appears at low temperature below 40 K. More direct observation was possible near 10 K. One important thing in our

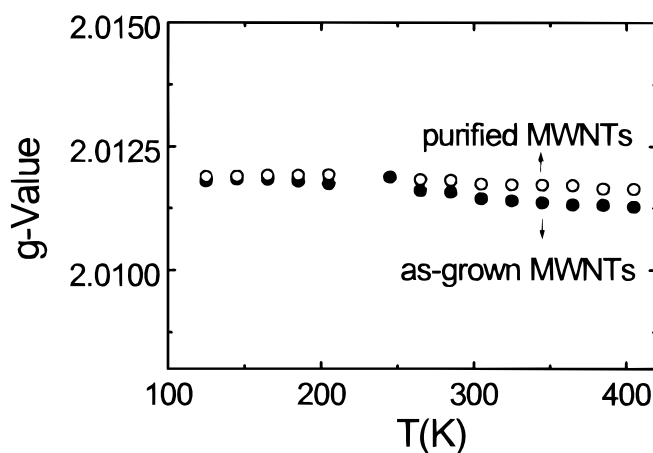


Figure 2. The temperature dependence of g value for (a) unpurified CNTs and (b) purified sample. The g -value of the CNTs after purification showed a nearly constant value in measuring temperature range, as compared to that of the unpurified one.

thick-film MWNT system is that the resistivity data follow the general hopping law expression in $\ln \rho \propto (T_0/T)^x$ with an exponent x changing from 1/4 to 1/2.

It is accepted that a steeply increasing resistivity of the highly conducting CNT can be explained as a weak localization of electrons in a metallic system in the low-temperature range of 10–50 K. Many authors have reported that at low temperatures the transfer of electrons between nearest-neighbor sites may be less favored than between more distant sites that are energetically accessible to reduce the energy necessary for the transition. The low-temperature transport properties of disordered systems are governed by VRH between the localized states. Mott was the first to predict the key relation for the temperature dependence of the conductivity for noninteracting carriers and for a constant density of states near the Fermi energy or a slowly varying function of energy. In disordered solids like our system of nonaligned MWNTs mixed with conductive paste, localized electrons can carry current at nonzero temperature but cannot screen the coulomb interaction as effectively as in metals. Coulomb interactions in a many-electron system always deplete the single-particle density of states $N(\epsilon)$ near the Fermi energy ϵ_F , relative to the noninteracting case.²⁸ For a barely insulating material, charge transport occurs via inelastic hopping between the states localized in both space and energy. Mott showed that at low temperature electrons seek accessible energy states by hopping distances beyond the localization length, leading to VRH conductivity $\sigma(T) \propto \exp(-T_0/T)^\nu$. For noninteracting electrons $\nu = 1/4$ in 3D, Efros and Shklovskii argued that including coulomb interactions, the ground state is stable with respect to a one-particle excitation only if $N(\epsilon)$ has a quadratic dependence on ϵ near ϵ_F

$$N(\epsilon) = \frac{3}{\pi} \left(\frac{\kappa}{e^2} \right)^3 (\epsilon - \epsilon_F)^2 \quad [1]$$

where κ is the dielectric constant. Because $N(\epsilon)$ vanishes only at ϵ_F , there is a “soft” coulomb correlation gap with a width $\Delta_c = e^3 (N_0/\kappa^3)^{1/2}$, where N_0 is the noninteracting density of states. In general, a power law $N(\epsilon) \propto (\epsilon - \epsilon_F)^m$ results in a hopping exponent $\nu = (m + 1)/(m + 4)$ as $T \rightarrow 0$, so that Eq. 1 gives $\nu = 1/2$. When T is high enough for a hopping electron to explore an energy range $k_B [T^3 T_0]^{1/4} > \Delta_c$, where $T_0 = 18/k_B \xi^3 N_0$ and ξ is the localization length, the influence of the coulomb gap can be neglected and the $\nu = 1/4$ exponent is expected. However, below the temperature $T_x = 0.38 e^4 \xi N_0 / k_B \kappa^2$, only states inside the gap are accessible and a crossover to $x = 1/2$ is predicted. This ES theory well fits the present resistivity data, as shown in Fig. 4a, suggesting the presence of a coulomb gap for about $T < 10 \pm 4$ K and a transition to a nearly insulating state. Note that this is the difference between pure CNT sheet (or mat) and our system mixed with conductive epoxy.

Considering previous reports, particularly regarding disordered metals and some doped inorganic semiconductors,²⁹ our observation is not peculiar. Efros pointed out that because of long-range interactions between localized states, the density of states near the Fermi energy tends to go to zero, which yields a parabolic coulomb gap. In the last few years the crossover between Mott and ES hopping regimes as a function of temperature has been found experimentally.

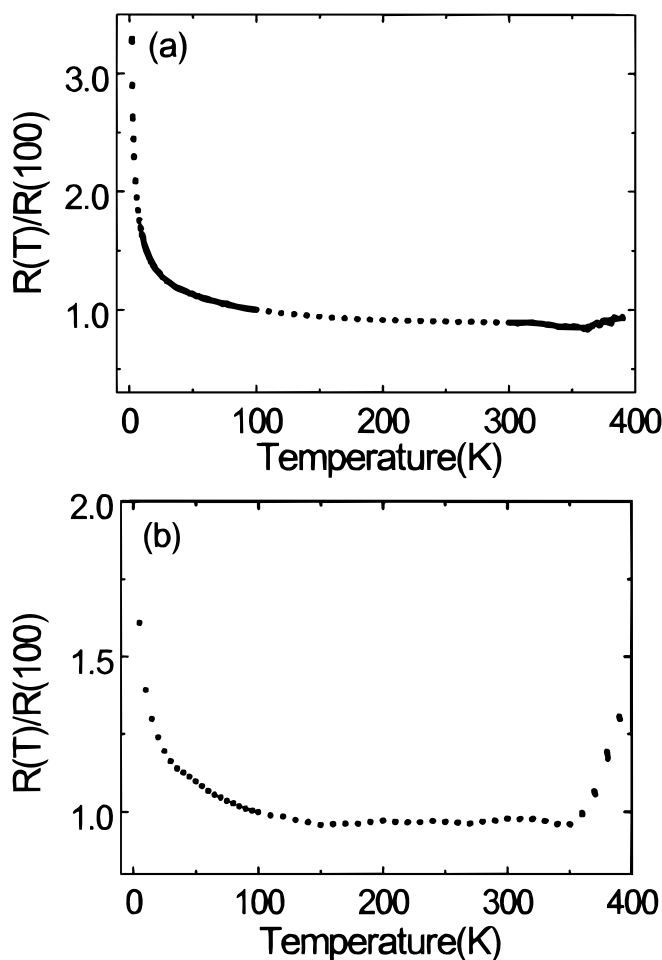


Figure 3. Log resistivity (R) vs. temperature for thick-film MWNTs. The resistivity of the MWNTs increases rapidly below 10 K.

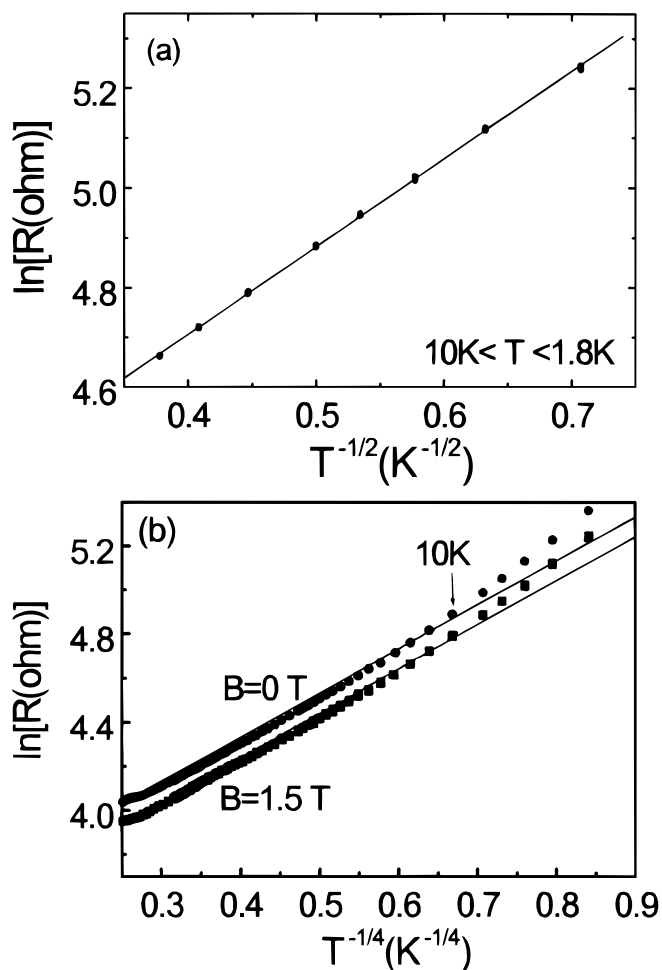


Figure 4. (a) Temperature dependence of the resistivity plotted as $\ln R$ vs. $T^{-1/2}$. The solid lines are the best-fit lines with VRH conduction as predicted by Shklovskii and Efros. (b) Temperature dependence of the resistivity of the thick-film MWNT plotted as $\ln R$ vs. $T^{-1/4}$. (—) Linear fits showing a large deviation with an increase of magnetic field.

Very recently, it has been observed that some conducting polymers and conducting polymer mixed with powder systems^{30,31} also show crossover from Mott to ES VRH conduction with a small coulomb gap. Here we would like to note that it is impossible to break up all the entanglements of the CNT materials with the conductive binder by the dispersion process used in our work and to remove all the other carbonaceous materials, although the ultrasonic and the subsequent intensive grinding process of the mixed paste leads to an improvement of the dispersion of the CNTs in the binder. Therefore, our thick-film MWNT samples show one of the characteristics of a disordered system and at the same time, it should be noticed that these phases form a conductive three-dimensional network throughout the whole sample as confirmed in resistivity measurements.

For the occurrence of a transition from the Mott to the Efros mechanism below 10 K, we can explain the effect as follows. The competition between the interaction between electrons and the disorder of the system results in glassy dynamics that are often associated with very long relaxation times. A very recent report revealed that in the presence of strong disorder, electrons could indeed have very long relaxation times.³² This occurs in a system with randomly placed electrons that have coulomb interactions. Heavily doped semiconductors and disordered metals like our thick-film MWNT system are assumed to be examples of such systems. The coulomb interaction between the localized states results in a so-called coulomb gap in the single particle density of states that is centered at the Fermi energy. In order to produce the coulomb gap, electron rearrangement must occur and the associated hopping can involve very long time scales. These long relaxation times are consistent with recent reports³³⁻³⁵ on thin-film semiconducting and metallic films which have shown that in the presence of strong disorder the electronic systems can relax very slowly, and the dip in the conductance (or rapid increase of resistivity) and the long relaxation times are present only at very low temperatures ($T < 20$ K). As the number of phonons increases with temperature, there is an increase in the phonon-assisted hopping of electrons. This leads to a rapid rearrangement of electrons on time scales that are too short to observe experimentally. As a result, no dips in the conductance or resistance were seen experimentally at higher temperature and in our case, above about 10 K.

Figure 5a shows the magnetic field dependence of the resistivity, showing a negative magnetoresistance $[R(H)-R(0)]/R(0)$ at lower fields in the temperature range 9–50 K. We can observe an effect at low temperatures 9–14 K, where the MR shows a quadratic dependence on magnetic field (H) and when replotting, as shown in the inset of Fig. 5b as a function of H^2 , the $[R(H)-R(0)]/R(0) \equiv \Delta R/R(0)$ are linear up to near 0.14 T at the low temperatures 9–14 K. The magnitude of $\Delta R/R(0)$ showed a minimum value and the sign was changed under a high magnetic field about 3 T. Increasing the temperature causes a shift toward lower magnetic fields, so that for temperatures near 50 K this minimum lies below 2 T. Recently, many groups report a linear negative MR or a quadratic MR, and it was suggested that a quadratic MR is negative in the case of strong disorder and positive in the case of weak disorder in the weak magnetic field limit. In our case, the weak magnetic field limit turns out to be about 0.14 T. The ways that the magnetic field affects the localized states and the hopping process are to change the transmission probability of tunneling between two states due to quantum interference effects and the change of the energy of the localized states via a Zeeman shift. The electron hopping probability under the magnetic field depends on the relative orientation of the two localized states and increase as they are aligned in the same direction, reducing the probability of antiparallel singly occupied spin states and resulting in a decrease of the hopping rates. These give rise to a change from a negative MR to a positive MR.

Finally, the field electron emission properties under a strong electric field were measured on the thick-film form of MWNTs on a soda-lime glass substrate predeposited with Cr lines for the cathode electrodes. The spacing between ZnO:Zn phosphor-coated ITO glass and the MWNT cathode was fixed at 100 μm using glass fiber spac-

ers. Before obtaining field emission data, we examined the surface of the thick-film MWNTs to check the occurrence of any cracking area and we stressed the samples several tens of times to stabilize the system. The measurements were performed at a pressure of 2×10^{-6} Torr. The plots of the emission current vs. electric field for two kinds of thick film systems with an external diameter of 10–15 nm and 20–30 nm are shown in Fig. 6a. These characteristics are relatively stable and repeatable without degradation of the background

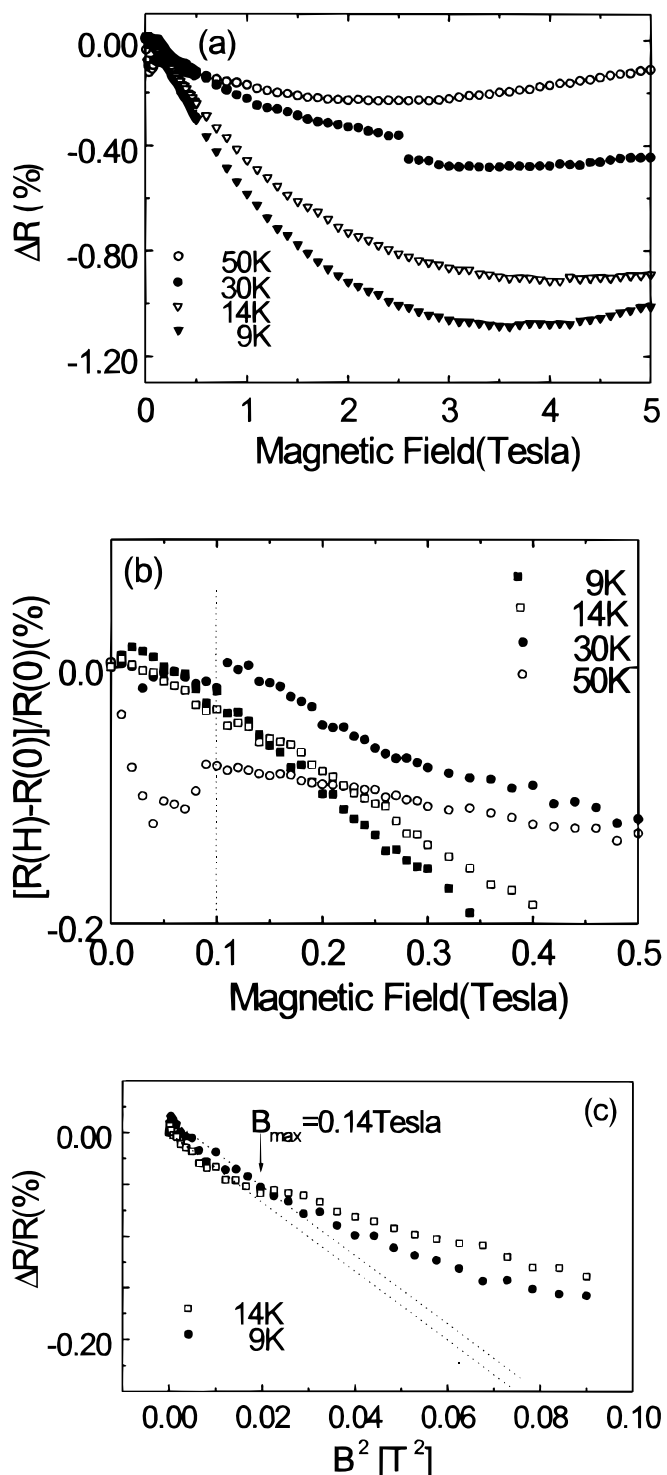


Figure 5. (a) The change of resistivity as a function of applied magnetic field and (b) magnetoresistance for different temperatures. (c) Shows the quadratic dependence of the resistance on the magnetic field in the weak field limit at 9 and 14 K, respectively.

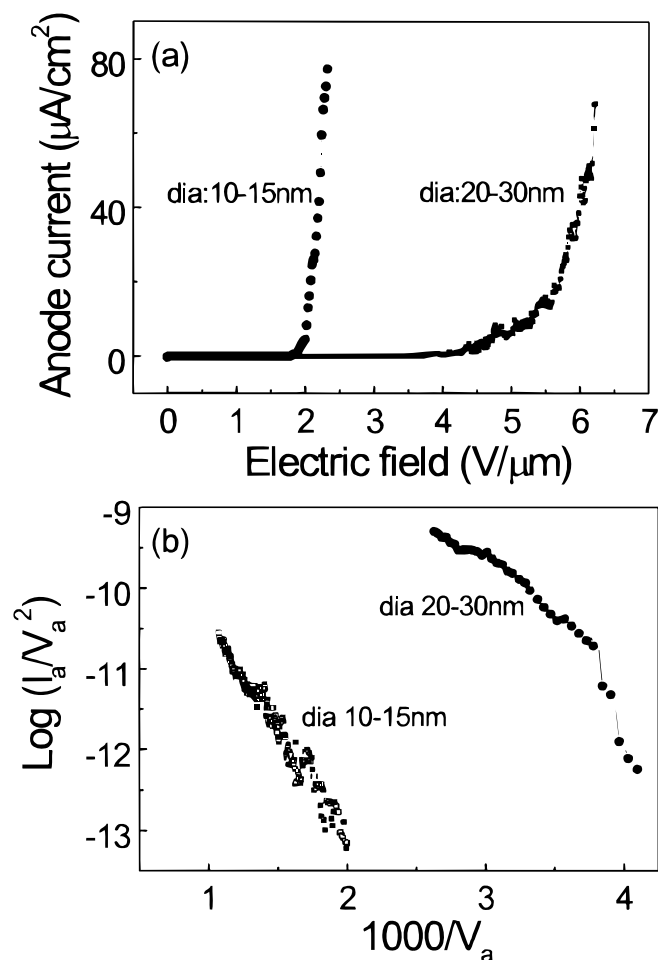


Figure 6. (a) Emission current–electric field characteristics and (b) F-N plots for thick-film MWNTs.

vacuum. The nominal onset fields for an emission current in Fig. 6a are 2.0 and 4.5 $\text{V}/\mu\text{m}$, depending on the diameter of MWNTs. Furthermore, the figure indicates that the lower value of the resistivity for the sample with the decrease of the diameter was closely related to the lowering onset field of electron emission. The I - V data plotted according to the typical Fowler-Nordheim (F-N) relationship for field emission is shown in Fig. 6b and fitted well. Although thick-film MWNT films are a strongly disordered system mixed with conductive epoxy, the metallic behavior provides a low turn-on field (1.5–4.5 $\text{V}/\mu\text{m}$) as well as a high emission current required for the field emission displays.

Conclusions

In this work, the results of ESR measurements and electrical conduction characteristics in a thick-film form of MWNT mixed with conductive epoxy were reported. The main focus of this paper was to compare the similarity and the difference between an individual MWNT (or sheet form pure MWNT) and CNT-binder composites system. As a result, we obtained evidence for metallic properties of our thick-film MWNT system through ESR study. The behavior of the resistivity of MWNTs for temperatures of 10–390 K indicates that our system is intrinsically metallic and the main contribution to the conductivity comes from carriers that hop directly between localized states via VRH. The temperature dependence above 10 K is in good agreement with that of an individual MWNT. However, with

the decrease of temperature below 10 K, the charge carriers in the system are localized by strong disorder, bringing a nearly insulating state as like metal-insulator transition. The behavior in the low-temperature regime can be explained by the ES conduction theory based on a strongly disordered system. Possible sources for the disorder are not confirmed at this moment; however, it is probable that the entanglement of the CNT system and binder effect contribute a localization effect on the carriers. Using the thick-film MWNTs for a large area display resulted in a very bright light as well as a very low turn-on field just like individual MWNTs at room temperature.

Acknowledgments

We thank Dr. il-Woo Park and Young-Wun Kang at the Korea Basic Science Institute for continuous help in performing the measurements. One of the authors (Y.-H.L.) is grateful to Jae-Eun Yoo at Iljin Co. in Korea for providing raw CNT materials.

Korea Institute of Science and Technology assisted in meeting the publication costs of this article.

References

1. S. Iijima, *Nature*, **354**, 56 (1991).
2. A. G. Rinzer, J. H. Hafner, P. Nokolae, L. Lon, S. G. Kim, D. Tomane, P. Nordlander, D. T. Golber, and R. E. Smalley, *Science*, **269**, 1550 (1995).
3. Y. Saito, K. Hamaguchi, T. Nishino, K. Hata, K. Tohji, A. Kasuja, and Y. Nishima, *Jpn. J. Appl. Phys., Part 2*, **36**, L1340 (1997).
4. Y. Saito, K. Hamaguchi, K. Hata, K. Uchida, Y. Tasaka, F. Ikazaki, M. Yumura, A. Kasuya, and Y. Nishima, *Nature (London)*, **389**, 554 (1997).
5. P. G. Collins and A. Zettl, *Phys. Lett.*, **69**, 1969 (1996).
6. P. G. Collins and A. Zettl, *Phys. Rev. B*, **55**, 9391 (1997).
7. Yu. V. Gulyacv, F. Zakharchenko, Z. Ya. Kosakovskaya, L. A. Chernozalonskii, O. E. Glukhova, and I. G. Torgashiov, *J. Vac. Sci. Technol. B*, **15**, 422 (1997).
8. Q. H. Wang, T. D. Corrigan, J. Y. Dai, R. P. Chang, and A. R. Krauss, *Appl. Phys. Lett.*, **70**, 3308 (1997).
9. Q. H. Wang, A. A. Setlur, J. M. Lauerhaas, J. Y. Dai, E. W. Seelig, and R. P. H. Chang, *Appl. Phys. Lett.*, **72/22**, 2913 (1998).
10. T. W. Ebbesen, H. J. Lezec, H. Hiura, J. W. Bennett, H. F. Ghaemi, and T. Thio, *Nature*, **382**, 54 (1996).
11. S. J. Tans, M. H. Devoret, H. Dai, A. Thess, R. E. Smalley, L. J. Geerligs, and C. Dekker, *Nature (London)*, **386**, 474 (1997).
12. D. H. Cobden, M. Bockrath, P. L. McEuen, A. G. Rinzier, and R. E. Smalley, *Phys. Rev. Lett.*, **81**, 681 (1998).
13. A. Bezryadin, R. M. Verschueren, S. J. Tans, and C. Dekker, *Phys. Rev. Lett.*, **80**, 4036 (1998).
14. S. Frank, P. Poncharell, Z. L. Wang, and W. A. de Heer, *Science*, **20**, 1744 (1998).
15. A. Bachtold, M. Henny, C. Terrier, C. Strunk, C. Schönenberger, J.-P. Salvetat, J.-M. Bonnard, and L. Forró, *Appl. Phys. Lett.*, **73**, 274 (1998).
16. S. N. Song, X. K. Wang, R. P. H. Chang, and J. B. Kettlers, *Phys. Rev. Lett.*, **72**, 697 (1994).
17. W. A. Heer, W. S. Bacsá, A. Chatelin, T. Gerfin, T. R. Humphery-Baker, L. Forró, and D. Ugarte, *Science*, **268**, 845 (1995).
18. B. Wei, R. Spolenak, P. K. Redlich, M. Ruhle, and E. Arzt, *Appl. Phys. Lett.*, **74/21**, 3149 (1999).
19. Y. Yoshida and I. Oguro, *J. Appl. Phys.*, **83**, 9, 4985 (1998), and other references therein.
20. Y. Yoshida, *J. Phys. Chem. Solids*, **60**, 1 (1999).
21. O. Zhou, R. M. Fleming, D. W. Murphy, C. H. Chen, R. C. Haddon, R. C. Ramirez, and S. H. Glarum, *Science*, **263**, 1744 (1994); M. Kosaka, T. W. Ebbesen, and H. Tanigaki, *Chem. Phys. Lett.*, **225**, 161 (1994).
22. G. Feher and A. F. Kip, *Phys. Rev.*, **98**, 337 (1955).
23. M. Dubois, A. Merlin, and D. Billaud, *Solid State Commun.*, **111**, 571 (1999).
24. F. J. Dyson, *Phys. Rev.*, **98**, 934 (1955).
25. R. J. Elliot, *Phys. Rev.*, **96**, 216 (1954).
26. N. F. Mott, in *Metal-Insulator Transitions*, 2nd ed., Taylor & Francis, London (1990).
27. N. F. Mott and E. A. Davis, in *Electronic Processes in Non-Crystalline Materials*, Oxford University Press, New York (1971).
28. B. I. Shklovskii and A. L. Efros, in *Electronic Properties of Doped Semiconductor*, Springer-Verlag, Berlin (1984).
29. A. Tiwari and K. P. Rajeev, *Solid State Commun.*, **109**, 119 (1999).
30. M. Ghosh, A. Barman, S. K. De, and S. Chatterjee, *Synth. Met.*, **97**, 23 (1998).
31. Y. O. Yoon, M. Reghu, D. Moses, A. J. Heeger, Y. Cao, T. A. Chen, X. Wu, and R. D. Rieke, *Synth. Met.*, **75**, 229 (1995).
32. C. Yu, *Phys. Rev. Lett.*, **82/20**, 4074 (1999).
33. Z. Ovadyahu and M. Pollak, *Phys. Rev. Lett.*, **79**, 459 (1997).
34. A. Vaknin, Z. Ovadyahn, and M. Pollak, *Phys. Rev. Lett.*, **82**, 669 (1995).
35. G. Martínez-Arizala, G. Martínez-Arizala, C. Christiansen, D. E. Grupp, N. Markovic, A. M. Mack, and A. M. Goldman, *Phys. Rev. B*, **57**, 12670 (1998).